Dipolar-interaction-induced fractal pattern formation in magnetic multilayers

F. Yang and F. Pan
Laboratory of Advanced Materials, Department of Materials Science and Engineering, Tsinghua University, Beijing 100084, People's Republic of China

(Received 5 April 2001; published 22 October 2001)

Models concerning particle diffusion and aggregation have been proposed for decades, and the aggregations with long-range dipolar interaction are simulated and analyzed numerically. In this paper, fractal clusters composed of particles diffusing with dipolar interaction are observed, and a model taking both magnetic force and diffusion activation energy into account is presented. The computer-simulation results generate clusters similar to those observed. And the measured sizes and dimensions of the experimental results are close to that of simulation. Further investigations on the magnetic energy and cluster size reveal that the dipolar interaction and thermal disruption play significant roles in the aggregation of nanosize magnetic particles and the interaction energy is the main driving force of the formation of the ordered structure.

DOI: 10.1103/PhysRevE.64.051402 PACS number(s): 61.43.Hv, 05.45.Df, 75.10.−b, 36.40.Cg

I. INTRODUCTION

The aggregation process of initially dispersed particles to form a fractal pattern has been of great interest during the last few decades. With the development of computer models, many theoretical works have focused on investigating the geometric and statistic properties of fractal clusters. In addition, the aggregation processes of naturally formed clusters or artificially induced aggregations are studied with a computer. There are two basic models of fractal aggregation: one is particle-cluster aggregation PCA, for instance, the diffusion-limited aggregation (DLA) model of Witten and Sander [1]; the other is cluster–cluster aggregation (CCA) [2,3]. However, since most of these models only considered a simple short-range interparticle interaction, they failed in describing the aggregation with long-range interparticle forces widely existing in nature.

To investigate the aggregation process with dipolar interaction, computer models have been set up to extend the aggregation models in order to include dipolar interparticle interactions [4]. The process is a contest of dipolar interaction, which favors an ordered structure, and thermal diffusion that induces chaotic aggregates. Two kinds of models concerning the dipolar-interaction-related aggregation are proposed: one is CCA, and the other is PCA. Both kinds of models give the results of more ordered structures than random aggregation. Besides, the fractal dimension D_f tends to shrink as the result of dipolar interaction [5].

On the other hand, experiments of dipolar interaction were performed in various CCA systems, most of which concerns the spatial configuration of magnetic microspheres in fluid systems. Particle association in magnetic fluids was observed directly [6,7], and the observed pattern results agree well with the theoretical simulation [7]. Yet in no experiment has the PCA process with dipolar interactions been observed, although computer models and systematic theoretical analysis were done years ago [5,8].

In this work, we investigate the particle aggregation with dipolar interaction in Fe/Tb multilayers. The observed patterns show some features that have been predicted by early PCA models. An adjusted PCA model is presented and computer simulations are performed to interpret the experimental phenomenon. In this model, particles are set to diffuse on the film plane where the activation energy of diffusion as well as magnetic interaction influences the aggregation process. Simulation results confirm that long-range magnetic interaction and the lattice binding to particle diffusion are decisive in determining the shape of fractal patterns.

II. EXPERIMENTS

The Fe/Tb multilayers were prepared by depositing alternatively pure Fe (99.999%) and Tb (99.99%) on freshly cleaved NaCl single crystals in a vacuum chamber with a vacuum of 5×10^5 Pa. The deposition rates were 0.03 nm/s for Fe and 0.09 nm/s for Tb. The total thicknesses of the films were 70–80 nm. The first layer on the substrate was terbium and the surface layer was iron.

After deposition, a metallurgical microscope was used to investigate the surface morphologies. Self-supporting films were prepared by first dissolving the NaCl substrate with deionized water and collecting it on copper grids for transmission electron microscope (TEM) observation and x-ray energy diffraction spectrum (EDS) analysis. The periodicities and crystalline structures of the films were analyzed by x-ray diffraction (XRD).

Both XRD and TEM analysis show that the multilayers were composed of Fe and Tb phases, and no intermetallic compounds or oxides formed. The microscope observation indicated that patterns were on the film surface. Immediately after the deposition, the films were identically even, composed of numerous nanocrystals in the TEM observation, and no special patterns were observed by a microscope. After 60 days kept at room temperature, the morphologies of the multilayers had changed a lot. Dendritelike patterns clearly observed under a microscope, protruded out of the film surface. Since the top layer of the multilayer is composed of iron, the patterns should be composed of Fe particles. EDS analysis confirms that the particles had more Fe concentration than that of the film area where no special pattern existed. Some of the particles may be iron oxide indeed, yet both iron and

iron oxide are ferromagnetic, so we treat the particle ferromagnetically in the simulation model.

The photographs taken by microscope are analyzed by an image analyzing computer with an output form of a 1024 $\times$1024 pixel matrix. When analyzing the fractal patterns observed in the multilayers, we use the radius-gyration method [9] to calculate the fractal dimension D_f of the pattern. The value D_f is determined from a log-log plot of the radius of gyration $R_g(N)$ as a function of the number of particles in the cluster N, by using the equation [9]

$$R_g(N)=\left(\frac{1}{N}\sum_{i=1}^{N} R_i^2-\frac{(\Sigma_{i=1}^{N}R_i)^2}{N^2}\right)^{1/2}\approx N^{1/D_f}. \qquad (1)$$

To investigate the origin of the patterns, an adjusted PCA model with dipolar interaction is established and computer simulations are conducted. By means of simulation, we deduce that the aggregation of magnetic particles with dipolar interaction induced the particle aggregation.

III. SIMULATION MODEL AND RESULTS

The simulation is a two-dimensional (2D) off-lattice [10] one, which has the width ranging from 2000 to 80 000 unit length. The lattice unit, or lattice constant, has its specific meaning in this model, i.e., one lattice unit is set to be equal to the diameter of the particle. Thus for simulations of different-size particles, the lattice is actually not the same in length. Particles of diameter d and magnetic moment $\boldsymbol{\mu}=\mu\mathbf{u}$ are set to diffuse and aggregate in the lattice, with μ being the magnetic-moment strength of a particle and $\mathbf{u}$ a unit vector oriented along its direction. The long-range magnetic interaction between two particles i and j separated by the distance $\mathbf{r}_{ij}=\mathbf{r}_i-\mathbf{r}_j$ ($\mathbf{r}$ is the vector on simulation plane) is

$$U_{ij}=\mu^2 E_{ij}, \qquad (2)$$

where E_{ij} is the dipolar energy

$$E_{ij}=\{\mathbf{u}_i\cdot\mathbf{u}_j-3(\mathbf{u}_i\cdot\mathbf{r}_{ij})(\mathbf{u}_j\cdot\mathbf{r}_{ij})/r_{ij}^2\}/(a_0 r_{ij})^3. \qquad (3)$$

Aggregation is started from a particle, referred to as the ''seed,'' placed at the origin of coordinates, bearing a randomly oriented 2D vector $\mathbf{u}_0$. The following particles are released from a randomly chosen position on a circle of radius R_{shot} centered on the seed. Each released particle is assigned a randomly oriented vector $\mathbf{u}_i$. The particle then becomes the walker, which would walk randomly in any direction with a step of one lattice constant until it either contacts the cluster or moves away from the origin a distance greater than R_{in}. In the latter case, the walker is removed and a new walker is released from the circle with radius R_{shot}. To reduce possible heterogeneous growth of the cluster [11], R_{shot} is set to be twice the largest distance of the particle from the origin, and R_{kill} is set to be R_{in} plus five lattice constants.

As other models concerning magnetic materials show, the random diffusion of walker is affected by the interactions exerted by the particles already attached to the cluster [8]. However, it is quite different from fluid systems, where the particles can diffuse with none or neglectable hindrance. In our case, iron particles diffuse on the film surface, affected by E_{lattice}, the diffusion activation energy exerted by the lattice match between particle and the underlying layer. Since the substrate of the walking particle is a terbium layer, it is assumed that the diffusing is homogeneous. Using the energy change as a calibration of diffusion probability, we calculate the total interaction energy between the walker and each attached particle before and after a possible walk of one lattice unit; the change in energy due to the movement is $\Delta E=E_{\text{new}}-(E_{\text{old}}+E_{\text{lattice}})$. If $\Delta E<0$, the movement is accepted and performed. If $\Delta E>0$, the movement is accepted with the probability

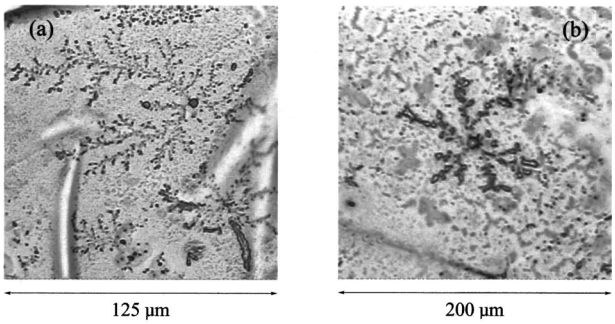

FIG. 1. Fractal patterns observed on Fe/Tb multilayers. (a) $[\text{Tb}(4.7\,\text{nm})/\text{Fe}(1.4\,\text{nm})]_{27}$ (sample A) and (b) $[\text{Tb}(2.1\,\text{nm})/\text{Fe}(4.3\,\text{nm})]_{25}$ (sample B).

$$p=\exp(-\Delta E K_{\text{dd}}), \qquad (4)$$

where the dimensionless parameter K_{dd} characterizes the dipole–dipole interaction plus the diffusion of iron particles relative to the disruptive thermal energy:

$$K_{\text{dd}}=-\frac{\mu^2}{d^3 k_B T}=\frac{\pi^3}{36}\frac{M^2 d^3}{k_B T}. \qquad (5)$$

The parameters in Eq. (5) are set according to experiment. The average particle diameter d (also assuming the simulation lattice constant) is set to be about 1.4 nm (the thickness of the Fe layers) for $[\text{Tb}(4.7\,\text{nm})/\text{Fe}(1.4\,\text{nm})]_{27}$ (sample A) and 4.3 nm for $[\text{Tb}(2.1\,\text{nm})/\text{Fe}(4.3\,\text{nm})]_{25}$ (sample B), respectively. The magnetization of iron particles is set to be 1.71×10^6 A/m [12]. The activation energy of lattice diffusion E_{lattice} is set to be 0.5 eV per atom.

After each step of walk, the walker experiences a magnetic-moment relaxation, i.e., it reorients in the direction of the total field on its position. If the walker attaches the cluster, i.e., the distance between walker and a certain fixed particle is smaller than the diameter d, the walker is reset to that point in its trajectory where it first contacts the fixed particle. Then, the walker is relaxed and becomes part of the cluster. The next step is the releasing of a new walker.

We simulated the clusters with $d=1.4$ nm for sample A and $d=4.3$ nm for sample B, respectively. Figure 1 shows the photos taken by microscope and Fig. 2 shows the simulation results.

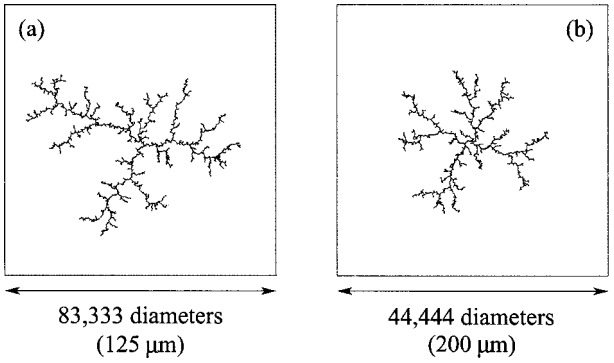

FIG. 2. Computer simulated clusters. The lengths noted in parentheses represent the calculated actual length, (a) total 60 000 particles, $d=1.4$ nm (sample A) and (b) total 30 000 particles, $d=4.3$ nm (sample B).

The particle number used in simulation is set in such a way that the generated cluster has close size to the experimental results. In total, 60 000 and 30 000 particles take part in simulations for samples A and B, respectively. Comparing the simulations with the experiment results, the similarity of morphologies is obvious. In Fig. 1, the fractal aggregates are assumed to consist of many small single domain particles, a similar case of which was observed by Liu and Ding [14]. In Figs. 1 and 2, we measure the fractal dimensions of both microscopic photos and simulated clusters by the radius-gyration method. The measured dimension of sample A is 1.38 ± 0.04 and the dimension of a corresponding simulated cluster is 1.38 ± 0.02, while the two values of sample B are 1.44 ± 0.06 and 1.46 ± 0.03, respectively. Both shapes and dimensions agree well between the simulated patterns and the microscopic photographs. In Fig. 1(a), the observed fractal is uneven in shape, because the particles are actually released in some neighboring sites, while they are released from far enough in simulation, shown in Fig. 2(a), and the heterogeneous growth is avoided [3].

IV. DISCUSSION

A. Range-limited dipolar interaction

It has been observed in liquid environments that magnetic particles aggregate in the driving of interaction force under zero-field conditions [6,7]. Similarly, the dipolar particles accumulate themselves by inner compellation. From the simulation, it can be seen that the magnetic interaction and the lattice binding are important in deciding the spatial configuration of magnetic particles. We now show how these two kinds of energy affect the diffusion process. The following calculations are carried out using the parameters of sample A, whose particles have diameter $d=1.4$ nm, i.e., the individual Fe layer thickness, and the simulation lattice has the length of 2000 constants.

First we consider the interaction of two particles separated by a large distance, one is the seed and the other walks near the lattice edge. The angles between magnetic-moment directions of the two particles and the x axis are θ_0 and θ_1, respectively. For convenience, their coordination are assumed to be (0, 0) and (1000, 0), respectively. From Eq. (4), the dipolar energy E_{01} of these two particles is

$$E_{01}=\frac{\cos(\theta_1-\theta_2)-3\cos\theta_1\cos\theta_2}{(1000d)^3}, \tag{6}$$

and the calculated magnetic interaction U_{01} is

$$U_{01}=\mu^2\frac{\cos(\theta_1-\theta_2)-3\cos\theta_1\cos\theta_2}{(1000d)^3}. \tag{7}$$

In our calculation, U_{01} is estimated to be no larger than 5×10^{-21} J, or 0.03 eV.

In contrast, the lattice limitation energy E_{lattice} is given by

$$E_{\text{lattice}}=E_0\left(\frac{d}{d_{\text{atom}}}\right)^3, \tag{8}$$

and the calculated E_{lattice} is about 2×10^3 eV, compared to which the dipolar interaction is negligible. Thus for distant particles, the diffusion is mainly controlled by lattice binding.

Nevertheless, if two particles are to be attached, e.g., the distance of them is about two lattice constants, the calculated U_{ij} is about $5\times10^{-13}J$, or 3×10^6 eV, i.e., eight orders larger than the above remote case. Yet the lattice limitation E_{lattice} is still 2×10^3 eV. In this case, the dipolar interaction is the most decisive. In experiments concerning hydrophobic magnetic nonoparticles deposited on a water subphase in a Langmuir trough, it was also found that small particles are organized in more compact aggregates than larger ones [13].

Our model shows that the magnetic interaction is strong for near particles and is omitable for remote particles. In other words, the short-distant array of particles is strongly affected by magnetic interaction.

B. Fractal structure relating to particle size

The two fractal patterns in the experiment are different in their shapes and dimensions, and this distinctness may be traced to the particle sizes. The simulations give confirming results. Equations (5) and (8) both have the item d, which means that not only the dipolar force but the thermal disruption and lattice binding are related to particle diameter. To investigate the influence of particle size on the fractal structure, several simulations are conducted with different particle diameter d, each have 2500 particles, as shown in Figs. 3 and 4.

Figure 5 shows the dimensions and coverage of these fractals. The dimension of every generated cluster is smaller than 1.715, which is the dimension of standard DLA [10]. The shrinkage in dimension results from the magnetic interaction between particles, as observed in other experiments [14,15]. Although all the simulations generate clusters composed of particles, the real meaning of particles is not the same for different d: one lattice constant, or one particle diameter, in reality represents different lengths for different simulations. We can see that the dimension (D_f) has the same variant tendency as the coverage (c) of particles. If particle diameters are larger than 1.0 nm, when d increases,

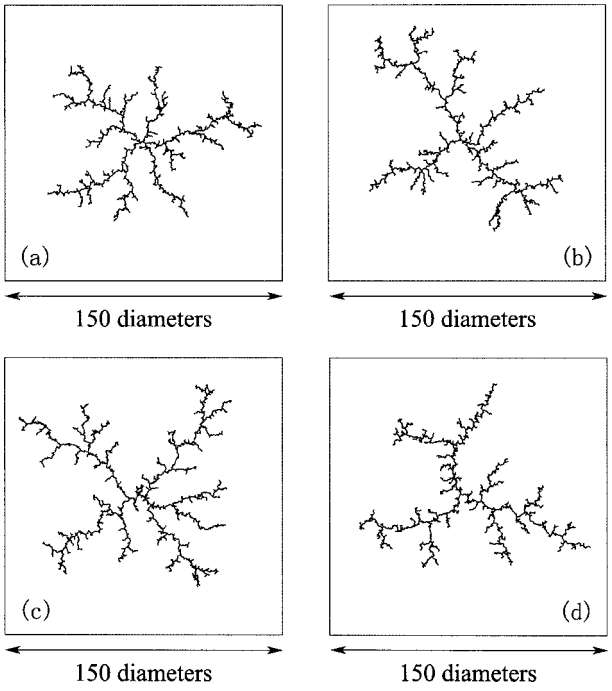

FIG. 3. Typical dipolar aggregates of 2500 particle, generated for several values of d. (a) $d=0.5$ nm, $D_f=1.44\pm0.03$, (b) $d=1.0$ nm, $D_f=1.38\pm0.02$, (c) $d=2.0$ nm, $D_f=1.42\pm0.02$, and (d) $d=5.0$ nm, $D_f=1.48\pm0.03$.

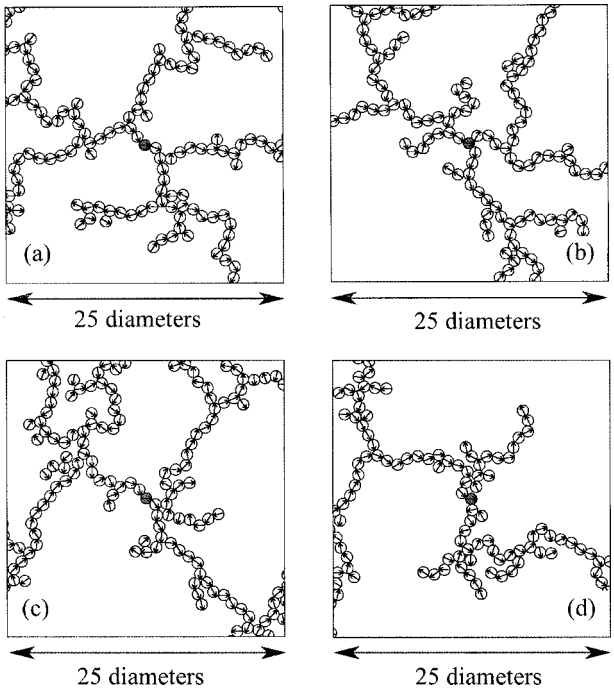

FIG. 4. Close-up view of the inner regions around the seed of the clusters shown in Fig. 3. The dipoles attached to each particle have been drawn in order to compare their arrangement. The central gray circle in each graph denotes the seed. (a) $d=0.5$ nm, (b) $d=1.0$ nm, (c) $d=2.0$ nm, and (d) $d=5.0$ nm.

D_f and c increase. In fact, the same length in the simulation lattice plane for different d may represent distinct lengths. Because the magnetic dipolar interaction becomes stronger when the distance between particles is smaller, and the strengthened interaction favors a more ordered structure [16], the magnetic force is stronger in the simulations with small d. In addition, the magnified aggregations (Fig. 4) near the seed show a more chaotic arrangement for particles with larger diameters. For the $d=1.0$ nm cluster, the particles are mostly arranged in single chains with highly oriented dipolar directions; in contrast, for the $d=5.0$ nm cluster, many particles are set in a disordered way; even some neighbor particles have opposite orientations. Another noting feature is that when d is 0.5 nm, the dipolar clusters have larger dimensions and coverage than those when $d=1.0$ nm. Thus factors other than dipolar interaction exert influence on the arrangement of magnetic particles.

C. System energy relaxation during the aggregation

The total interaction energy of all particle pairs is recorded during the simulation in order to investigate the system energy transition. As Fig. 6 shows, every aggregation is an energy reducing process, in which the energy relaxes in a rapid linear decay, accompanied with tiny fluctuations due to thermal noise. One should note that the dipolar interaction energies have orders of difference among simulations with different particle size due to different interaction distances as discussed before, yet the tendencies are the same. For a particle diameter of 0.5 nm, the dipolar interaction energy of the system is the strongest, i.e., about -7.0×10^4 eV when 2500 particles aggregate. Yet the system dipolar energy is only -70 eV when $2500d=5.0$ nm particles aggregated. Further, the total energy of dipolar interaction for a standard DLA aggregation is also calculated for comparison as shown by the dotted curves in Fig. 6 in which the magnetic moments are randomly assigned to each particle. One can see from Fig. 6 that the magnetic-energy-favor diffusion and relaxation of particles significantly reduce the system energy, while the standard DLA energy fluctuation (e.g., the enlarged curve of dipolar energy in DLA shown in Fig. 7) is almost indiscernible compared to the dipolar energy change in magnetic particle systems, i.e., the system dipolar energy has little change indeed.

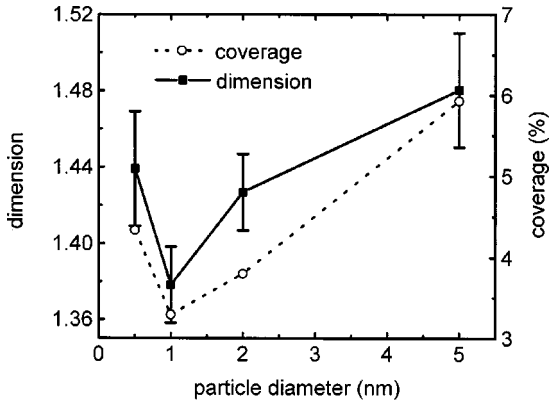

FIG. 5. Dimensions and coverage of the clusters shown in Fig. 3.

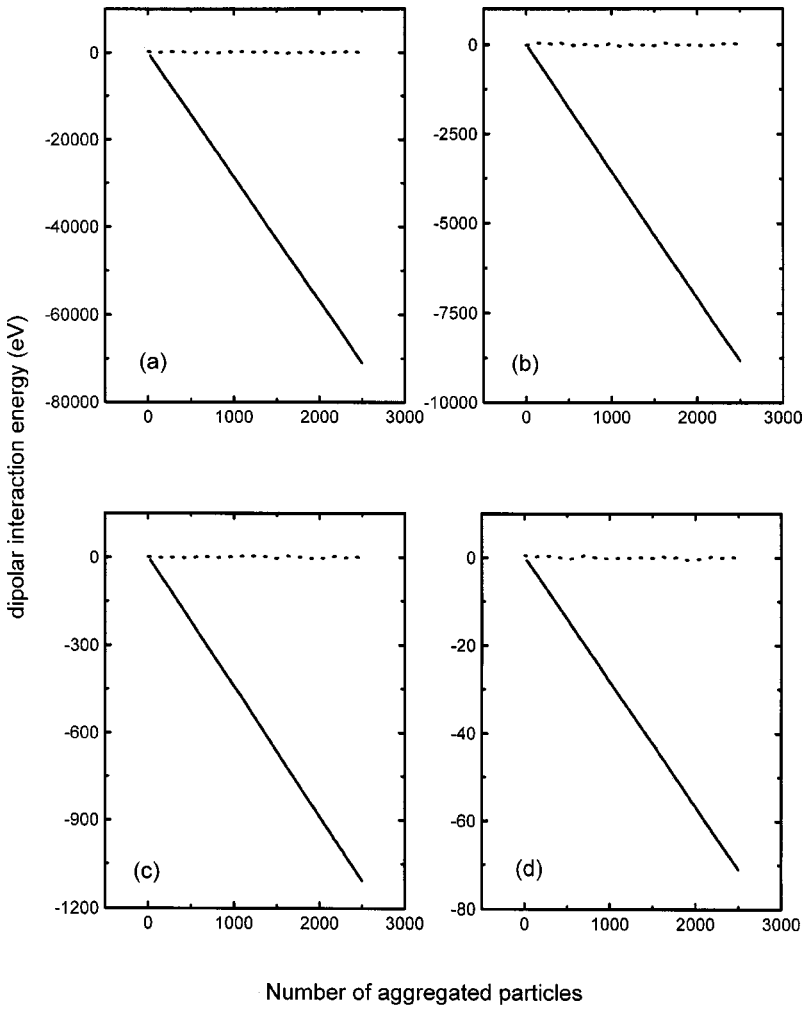

FIG. 6. Change of total dipolar energy during aggregation, of the simulation process. (a) $d=0.5$ nm, (b) $d=1.0$ nm, (c) $d=2.0$ nm, and (d) $d=5.0$ nm. The solid lines are the energy change for the model of dipolar interaction, and the dotted lines are the dipolar energy change for the standard DLA model.

For a more quantitative insight of the thermal disruption, the relationship between K_{dd} and the particle diameter d is investigated with the simulated results. From Eq. (5), $K_{dd}^{-1} \sim T$ can be interpreted as some kind of dimensionless temperature, related to the intensity of the interaction and presenting the thermal disturbance [5,7,8]. In Fig. 6, the slope of the energy reduction curve, $S=\Delta E/\Delta(\text{particle})$, represents the change of total dipolar interaction energy in unit time of particle aggregation. K_{dd} and S values are shown in Table I as the function of particle diameter. Since both are functions of particle diameter, SK_{dd} is calculated to be unrelated to particle diameter and it represents the relative strength of the dipolar interaction to thermal disruption, as shown in Fig. 8. This curve has a similar tendency as Fig. 5, which shows the dimensions and coverage of the clusters. Figure 8 clearly demonstrates that $d=1.0$ nm particles are the least diffusive. In addition, the well-aligned clusters in Fig. 4(b) also confirm this. And other-size particles are more mutable by thermal activation, even at the same temperature.

From the three sections of discussion, it is concluded that ordered assemblies of dipolar magnetic particles are governed by the influence of competing mechanisms, i.e., the interplay of dipolar interaction and thermal motion [8,17]. The result of such a competition is clearly shown in our simulation and also that the reducing of dipolar interaction

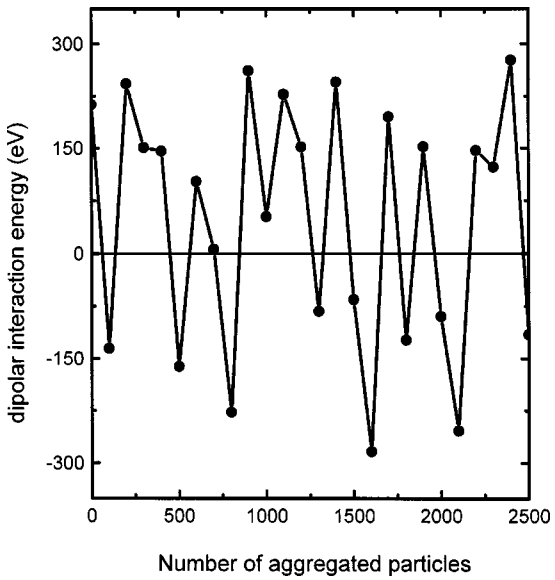

FIG. 7. Dipolar energy change for the standard DLA, in which the magnetic-moment directions are randomly assigned to each particle. Also, in an enlarged scale, the curve is shown in Fig. 6(a), where the particle size is 0.5 nm.

TABLE I. K_{dd} and S values as the function of particle diameter, based on the simulations shown in Fig. 3. S is deduced from the slope of system dipolar energy reduction curve in Fig. 7.

Particle diameter (nm)	S (eV/particle)	K_{dd}	SK_{dd}
0.5	28.354 51	24 204	686 293
1.0	3.540 77	193 637	685 624
2.0	0.444 49	$1.549\,1\times10^{6}$	688 558
5.0	0.028 46	$2.420\,46\times10^{7}$	688 864

energy is the main driving force of the formation of the ordered structure in dipolar interaction systems. For nanosize magnetic particles, the dipolar interaction is significantly stronger for smaller ones, while thermal motion also increases with reducing size. Yet when other factors are concerned, for instance, lattice binding energy as shown in this work, the former two competing mechanisms have a different changing rate and each favors a specific size range; thus a least diffusive state is likely to exist for a certain size of particle.

V. SUMMARY

Fractal patterns are observed on Fe/Tb multilayers and confirmed to be the clusters of ferromagnetic particle aggregation. To the film structure, a modified model is presented including the dipolar interaction between particles and lattice binding. Computer simulations with the new model generated clusters that have similar shapes and close fractal dimensions to those observed. Calculations show that the magnetic force is negligible compared with diffusion activation energy when the particles are separated by long distance, while it is dominant when the particles are near each other. Aggregation simulations for particles whose diameters range from 0.5 to 5.0 nm are conducted and show that the dipolar interaction is stronger when particle distance is getting closer. The dimension and coverage of $d=1.0$-nm clusters is the smallest, due to strong dipolar interaction and lattice binding. The energy change during the aggregation shows that the magnetic interaction energy is the main driving force of the formation of the ordered structure in dipolar interaction systems. The competing mechanisms of dipolar interaction and thermal disruption are likely to change their relative strength by other factors such as lattice binding.

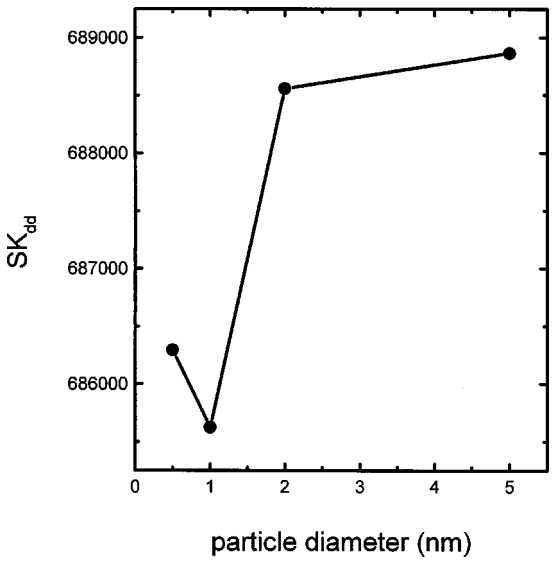

FIG. 8. Relative strength of dipolar interaction to thermal disruption, $S\,K_{dd}$ vs particle diameter. S is the slope of the energy curve shown in Fig. 6. The values are also listed in Table I.

ACKNOWLEDGMENTS

The authors are indebted to Professor B. X. Liu for his helpful discussions. The financial aid from the National Natural Foundation of China, the Ministry of Science and Technology of China through Grant No. G2000067207-1, and the administration of Tsinghua University are gratefully acknowledged.

[1] T. A. Witten and L. M. Sander, Phys. Rev. Lett. **47**, 1400 (1981); Phys. Rev. B **27**, 5686 (1983).
[2] P. Meakin, Phys. Rev. Lett. **51**, 1119 (1983).
[3] M. Kolb, R. Botet, and R. Jullien, Phys. Rev. Lett. **51**, 1123 (1983).
[4] P. Meakin and M. Muthukumar, J. Chem. Phys. **91**, 3212 (1989).
[5] R. Pastor-Satorras and J. M. Rubí, Phys. Rev. E **51**, 5994 (1995).
[6] L. Donselaar, P. M. Frederik, P. Bomans, P. A. Buining, B. M. Humbel, and A. P. Philipse, J. Magn. Magn. Mater. **201**, 58 (1999).
[7] W. J. Wen, F. Kun, K. F. Pál, D. W. Zheng, and K. N. Tu, Phys. Rev. E **59**, R4758 (1999).
[8] R. Pastor-Satorras and J. M. Rubí, Phys. Rev. Lett. **80**, 5373 (1998).
[9] T. Vicsek, *Fractal Growth Phenomena*, 2nd ed. (World Scientific, Singapore, 1992).
[10] S. Tolman and P. Meakin, Phys. Rev. A **40**, 428 (1989).
[11] P. Meakin, Phys. Rev. A **27**, 1495 (1983).
[12] D. Jiles, *Introduction to Magnetism and Magnetic Materials* (Chapman and Hall, London, 1991).
[13] S. Lefebure, C. Menager, V. Cabuil, M. Assenheimer, F. Gallet, and C. Flament, J. Phys. Chem. B **102**, 2733 (1998).
[14] B. X. Liu and J. R. Ding, Phys. Rev. B **40**, 7432 (1989).
[15] J. R. Ding and B. X. Liu, Phys. Rev. B **40**, 5834 (1989).
[16] G. Indiveri, A. C. Levi, A. Gliozzi, E. Scalas, and H. Möhwald, Thin Solid Films **284–285**, 106 (1996).
[17] R. Pastor-Satorras and J. M. Rubí, J. Magn. Magn. Mater. **221**, 124 (2000).